Title

Climate change impacts on groundwater storage in the Central Valley, California

Journal

Climatic Change, 157(3-4)

ISSN

0165-0009

Authors

Alam, Sarfaraz
Gebremichael, Mekonnen
Li, Ruopu
et al.

Publication Date

2019-12-01

DOI

10.1007/s10584-019-02585-5

Peer reviewed

Climatic Change (2019) 157:387– 406
https://doi.org/10.1007/s10584-019-02585-5

Climate change impacts on groundwater storage in the Central Valley, California

Sarfaraz Alam[1] · Mekonnen Gebremichael[1] · Ruopu Li[2] · Jeff Dozier[3] · Dennis P. Lettenmaier[4]

Received: 18 March 2019 / Accepted: 22 October 2019 / Published online: 26 November 2019

Abstract

Groundwater plays a critical supporting role in agricultural production in the California Central Valley (CV). Recent prolonged droughts (notably 2007–2009 and 2012–2016) caused dramatic depletion of groundwater, indicating the susceptibility of the CV's water supply to climate change. To assess the impact of climate change on groundwater storage in the CV, we combined integrated surface water and groundwater models with climate projections from 20 global climate models and thereby explore the vulnerability of CV groundwater under two climate scenarios RCP4.5 and RCP8.5. We found that groundwater has been declining over the past decades (3 km^3/year on average during 1950–2009). In the absence of future mitigating measures, this decline will continue, but at a higher rate due to climate change (31% and 39% increase in loss rate under RCP4.5 and RCP8.5). The greatest loss (more than 80% of the total) will occur in the semi-arid southern Tulare region. We performed computational experiments to quantify the relative contribution of future crop water use and headwater inflows to total groundwater storage change. Our results show that, without management changes, continuing declines in future groundwater storage will mainly be attributable to ongoing overuse of groundwater. However, future changes in the seasonality of streamflow into the CV, (small) changes in annual inflows, and increased crop water use in a warmer climate will lead to 40–70% more annual groundwater losses than the current annual average, up to approximately 5 km^3/year.

Keywords Groundwater · Central Valley · Climate change · Integrated modeling

Electronic supplementary material The online version of this article (https://doi.org/10.1007/s10584-019-02585-5) contains supplementary material, which is available to authorized users.

✉ Sarfaraz Alam
szalam@ucla.edu

Extended author information available on the last page of the article

1 Introduction

Global warming poses serious threats to water resources, particularly in the Western US (Gleick 2000). Climate change can directly and/or indirectly affect different components of the hydrological cycle, in which precipitation, snowmelt, and evapotranspiration are linked to agricultural water supply and demand (Garrote et al. 2015). Increases in water demand and decreases in surface water supply caused by a warming climate can negatively affect groundwater storage through increased groundwater exploitation, especially in regions like the Central Valley of California where groundwater is already stressed.

The Central Valley (CV) of California is one of the most productive agricultural regions in the world. On average, sources of irrigation water are about equally divided between surface water and groundwater (Li et al. 2018), but during droughts, surface water availability is reduced, and the difference is mostly made up by groundwater, along with some reduction in irrigated area to reduce demand. Throughout the CV, groundwater resources relative to surface water resources vary, partly due to the natural north-south precipitation gradients, with groundwater relatively more important to the south. Surface water comes mostly from streams that originate in the Sierra Nevada Mountains east of the CV (hereafter referred to as headwater watersheds). Precipitation is highly seasonal, mostly occurring from October through March. Pronounced spatial differences exist in terms of the amount and timing of surface water supplies from the headwater watersheds, arising from higher total precipitation in the north and greater winter snowpack storage in the south of the Sacramento-San Joaquin delta. To address these differences and the overall semi-arid climate, the CV relies on a complex network of reservoirs and manmade canals to store, import, and transfer water, especially to its driest southern parts.

In recent decades, a gap has widened between water demand and surface water supply, which was caused by reductions in water available from the Colorado River Basin, a shift from row crops to more water intensive crops, and pervasive droughts over much of the last decade. This gap has been mitigated mostly by the extraction of groundwater, along with the reduction in irrigated areas (Xiao et al. 2017). Overexploitation of groundwater was especially pervasive in southern part of CV. Concerning the long-term viability of agriculture in the CV and the dropping groundwater levels, California State Legislature enacted the Sustainable Groundwater Management Act (SGMA), which requires that groundwater use in the state be managed at sustainable levels (California State Legislature 2014).

Historically, the area devoted to irrigated agriculture in the CV expanded over a 100-year period from the 1870s to the 1970s, during which the areas under irrigation were roughly stable (Olmstead and Rhode 2017). However, except for exceptionally high runoff years, the water balance in parts of the CV has been in deficit (Xiao et al. 2017; Famiglietti 2014). This situation worsened during two drought periods in the past decade. Using satellite data from the Gravity Recovery and Climate Experiment (GRACE), Famiglietti et al. (2011) estimated that the CV experienced net groundwater depletion of about 20 km^3 during 2003–2010. Xiao et al. (2017) estimated cumulative groundwater storage change (ΔGW hereafter) using multiple data sources, including GRACE data and in situ records, and found a depletion rate of 7.2 ± 1.0 km^3/year from April 2006 to March 2010 and 11.2 ± 1.3 km^3/year for the 2012–2016 drought. Other relevant studies support similar findings that CV groundwater has been in decline at least in the past 50 years (e.g., Famiglietti et al. 2011; Scanlon et al. 2012), with most accelerated decline over the last decade. The loss of groundwater in recent droughts is a key

indicator of the susceptibility of the CV groundwater system to climate variability and change, to an extent that has not previously been estimated.

The objective of this study is to assess the historic changes in groundwater storage and to estimate the additional stress likely to be imposed by future climate change within CV over the next century. In general, there are two important factors that affect CV groundwater, these are (i) climate change, which has resulted in changes in headwater runoff patterns associated with earlier snowmelt and increased evaporative demand (VanRheenen et al. 2004) and (ii) crop evolution (change in crop area and patterns), resulting in increased crop water use (Alam et al. 2019). In this study, we disentangle these effects over the historic records and determine how much additional stress future climate may impose.

To address these issues, we use a suite of global climate model outputs archived for the Fifth Assessment Report of the Intergovernmental Panel on Climate Change (IPCC). We test projections both for modest global emissions increases (RCP4.5) and a more draconian scenario (RCP 8.5). Compared with previous efforts (e.g., Massoud et al. 2018; Hanson et al. 2012), we use a full suite of climate models and scenarios to represent future climate conditions that will affect CV groundwater in the coming decades. We use a hydrology model to represent the effects of headwater watersheds in producing streamflow into downstream reservoirs and subsequent releases from reservoirs that produce surface flows into the CV. Finally, we represent the implications of future surface runoff into the CV on groundwater use. Our domain is the entire Sacramento-San Joaquin-Tulare lowland and upland domain (SSJT, see Fig. 1), as described in the next section.

2 Study area

The study area consists of the entire CV from north of Redding to the Tulare River basin lowlands (see Fig. 1). In total, the study area encompasses approximately 160,000 km^2, around one-third of the area of California. Most of the CV is nearly flat or in low-relief, in contrast with the surrounded high-elevation headwater watersheds. Strong precipitation gradients characterize the transition from the valley floor to the mountains, and a subtler precipitation gradient exists from the humid north to the semi-arid south (Bales et al. 2006).

Averaged over the domain, more than 75% of the average annual precipitation occurs between October and March (Cooper et al. 2018). Notwithstanding that headwater basins to the south are more snow-dominated than those to the north, northern watersheds generate more than two-thirds of the total annual inflow to the CV. This imbalance has motivated the construction of dams and conveyance structures that transfer water from the north to the south. This complex network of surface storage and conveyance structures control the basin-wide surface water distribution throughout the year. The reservoirs store high winter and spring flows and release them during the high-demand summer season, while providing flood protection and environmental services (mostly supplementing summer low flows). There are around 18 major reservoirs located in headwater watersheds (shown in Fig. 1) and five major hydrologic regions (HR) in CV, including Sacramento (SC), San Joaquin (SJ), Tulare (TL), Delta, and East-Delta (Brush and Dogrul 2013). In this study, we compared groundwater storage changes in three major hydrologic regions: Sacramento, San Joaquin, and Tulare.

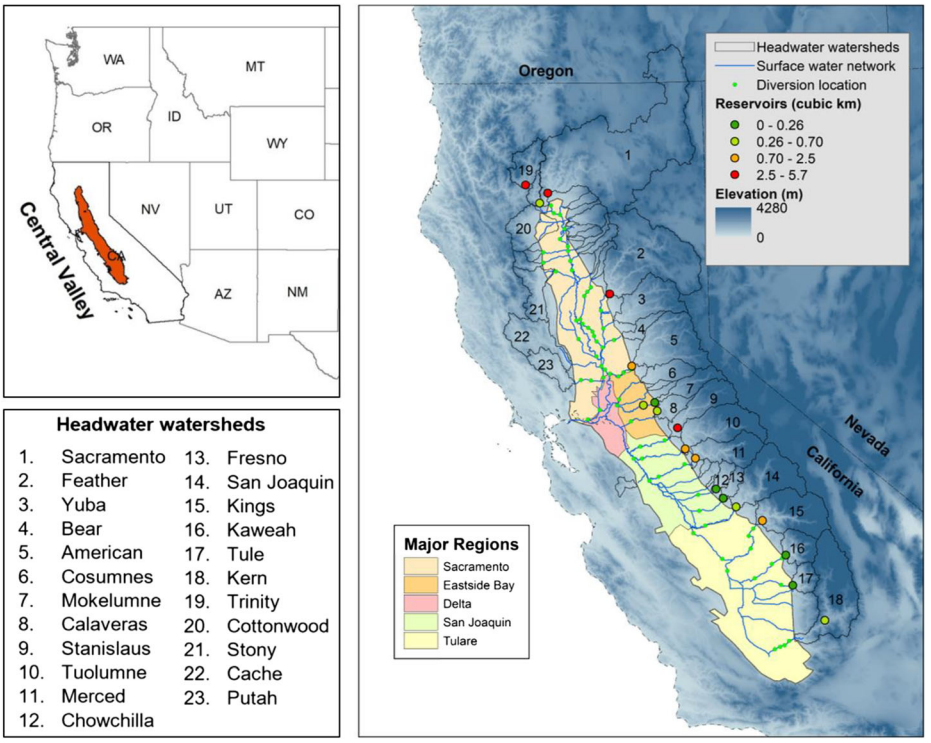

Fig. 1 Map showing Central Valley and its surrounding watersheds (headwater watersheds). The five major hydrologic regions and rivers flowing through them are shown in the map to the right. Headwater watersheds and major reservoirs we represent in the study region are also shown (right). Blue shades indicate elevations of headwater watersheds

3 Approach and data

3.1 Modeling approach

We used a range of climate model projections and hydrologic and water resources management models to evaluate groundwater storage changes in major hydrologic regions. In general, our headwaters-to-groundwater modeling framework can be divided into three major components, which include models representing the headwater watershed, headwater reservoir regulation, and integrated surface water-groundwater. We linked each of the components forced with different climate projections and scenarios. A conceptually similar modeling approach was taken by Hanson et al. (2012), which showed that such a model integration can effectively estimate potential changes in groundwater due to climate change over the CV. The steps we followed are to (1) identify representative climate models and extract downscaled climate variables; (2) simulate headwater watershed runoff using the Variable Infiltration Capacity (VIC) model (Liang et al. 1994); (3) model headwater reservoir storage and releases using a reservoir simulation model (CVmod: VanRheenen et al. 2004); (4) model the integrated surface water-groundwater system using the California Central Valley Groundwater-Surface Water Simulation Model (C2VSIM: Brush et al. 2013); and (5) assess historical and future change in groundwater storage in CV (Fig. 2).

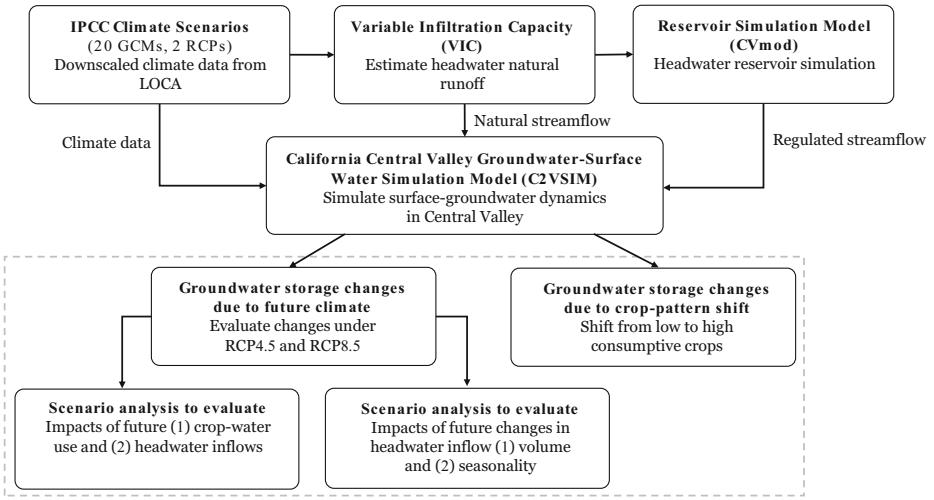

Fig. 2 Connectivity and flow of data in our integrated modeling system. Items in the dashed box are the key analysis and outputs

3.2 Headwaters to groundwater modeling framework

The headwater watersheds in our modeling framework are represented by the VIC model—a physically based semi-distributed hydrological model that solves the land surface water and energy budgets at the grid cell level (Liang et al. 1994). While there are other models like Noah-MP (Niu et al. 2011) and BCM (Flint and Flint 2007) that could be used to simulate headwater watershed hydrology, we selected the VIC model because it has a long history of success in numerous studies, including those conducted for the CV system (Van Rheenen et al. 2004; Xiao et al. 2017). For the current study, we used VIC simulations by Pierce et al. (2018) that are available at daily time step and 1/16th degree (6 km) spatial resolution for both historical (driven by the Livneh et al. 2015 gridded historical dataset of 6 km resolution) and future periods (driven by LOCA downscaled climate projection for 32 climate models by Pierce et al. 2014 at 6 km resolution). We obtained the VIC simulation data from the Cal-Adapt online portal (Cal-Adapt 2018). We aggregated VIC-simulated daily runoff to monthly to generate inflows to reservoirs and other CV inflow points. Hereafter, we refer to VIC-simulated headwater watershed flows as inflows to the CV, which are regulated by reservoirs (where they exist) or otherwise flow directly to the CV. To verify the accuracy of VIC-simulated headwater watershed flows, we compared annual flows from major watersheds with available unimpaired flow estimates (CDWR 2016). They are generally in agreement (see Table S1 and Fig. S1 in supplementary information). We then used the headwater inflows as inputs to the headwater reservoir model (where reservoirs exist) and surface water-groundwater model (in headwater watersheds without reservoirs).

We simulated headwater reservoir operation using the reservoir simulation model CVmod (Van Rheenen et al. 2004). CVmod operates at a monthly time step. The model takes natural inflows from surrounding headwater basins (observed or simulated by a hydrological model such as VIC) as inputs and simulates reservoir storage and releases based on operations related to flood control, hydropower production, navigation, instream flow requirement for fish, and water supply demands. We calibrated CVmod to historical reservoir operations (releases and

storage). We also extended the model to represent four additional reservoirs in the Tulare basin (Pine Flat, Isabella, Success, and Kaweah Lake), calibrated with historical flows, and evaluated performance relative to observed reservoir storage and releases. We ran CVmod using VIC simulated headwater inflows to obtain reservoir release and storage for both historical and future climate simulations (Fig. 1 shows reservoirs considered in this study). (Details of model performance are given in Text S2, Table S2 and Fig. S2 of supplementary information.)

We used C2VSIM to simulate CV surface water and groundwater dynamics. C2VSIM, originally developed by CDWR, has a long history of development and applications in climate change studies (Miller et al. 2009; Brush et al. 2013; Brush and Dogrul 2013; Dale et al. 2013). The model simulates groundwater flows in three layers on finite element grids and dynamically couples with a one-dimensional simulation of land surface hydrologic processes, streamflow, vertical movement in the vadose zone, lakes, and flows from adjacent ungauged watersheds (Brush and Dogrul 2013). The groundwater flow equations are solved at 1392 finite element grids (51,000 km^2) and land surface hydrologic processes are computed at 21 water balance sub-regions. We used a coarse grid version of the model with element sizes ranging from 5.4 to 87 km^2 (average 37 km^2). The model estimates water demand given irrigated land use as determined by agricultural management parameters, crop types, water supply from surface water diversions and groundwater pumping, and climatic forcing. Brush et al. (2013) calibrated C2VSIM for the period 1975–2003 to produce a good match between simulated and observed streamflow, groundwater heads, and head differences between wells. C2VSIM runs for the period October 1921 to September 2009 at a monthly time step (see Brush et al. 2013 for details). While there are other models like CVHM (Faunt et al. 2009) that could be employed for simulating groundwater processes, we selected C2VSIM because of (i) its greater temporal coverage for the current study and (ii) a long history of successful applications.

Among the many input data to C2VSIM, the ones we adjusted were precipitation, crop evapotranspiration (ETc), crop types, surface water diversions, urban water demand, and inflow from surrounding watersheds. To demonstrate the direct impacts of climate change on agriculture and groundwater resources, we set urban and agricultural land use patterns, and irrigation efficiency to 2003 values. However, given that urban water demand is anticipated to increase in the future (Johnson 2009), we applied a 1.2% annual rate of increase in urban water demand, similar to Hanson et al. (2012), from year 2000 through 2098. We computed ETc as the product of the crop coefficient (Kc) and reference crop evapotranspiration (ETo) following Allen et al. (1998). The mean values and seasonal variations in Kc are obtained from Brush et al. (2004) and ITRC (2003). We estimated ETo using the Penman-Monteith equation and following Allen et al. (1998) at 1/16-degree spatial resolution for the study region. This ETo calculation requires air temperature, vapor pressure deficit, relative humidity, solar radiation, and wind speed (Eq. 1).

$$ET_0 = \frac{0.408\Delta(\mathrm{Rn}-\mathrm{G}) + \gamma \frac{900}{\mathrm{T}+273} u_2 (e_s - e_a)}{\Delta + \gamma(1 + 0.34u_2)} \quad (1)$$

In Eq. 1, Rn is net radiation, G is ground heat flux (assumed zero), T is mean daily air temperature at 2 m height (°C), u_2 is wind speed at 2 m height, e_s is saturation vapor pressure, e_a is actual vapor pressure, Δ is the slope of the saturation vapor pressure curve, and γ is the psychrometric constant.

We extracted all the required variables over CV from the VIC model (driven by Livneh et al. 2015 data for the historical period and LOCA climate projections from Pierce et al. 2014) for the future. We temporally aggregated ETo to obtain monthly data from daily time series and extracted the sub-region averaged ETo. Twelve major crop types are used by C2VSIM including virtual crops that aggregate multiple actual crops (e.g., grains, orchard, field crops, truck crops). To verify that C2VSIM performed well during the historical simulation driven by the Livneh et al. (2015) data, we compared our groundwater storage change results with previous studies (shown in Section 4).

Additionally, C2VSIM requires user-defined surface water diversion information along the stream network (shown in Fig. 1). Previous studies of the CV and its contributing watersheds used relatively simple methods to estimate surface water deliveries. For instance, Hanson et al. (2012), Hanson and Dettinger (2005) estimated future diversions based historical analogs (partitioning years into wet and dry periods), and Miller et al. (2009) used historic diversion statistics (mean, median). We developed a simple linear programming (LP) model with surface water networks similar to C2VSIM to estimate surface water diversions (Fig. 1 showing the network and diversion locations; a more detailed description of the diversion locations is available in Brush and Dogrul 2013). The objective of the LP model is to maximize the surface water delivery under constraints like mass balance and maximum/minimum instream flows (see Text S3 of supplementary information). We used upstream headwater watershed flows as the upstream boundary to the LP model. We first ran the LP model at a monthly time step for the projection period and then applied the surface water diversion outputs to C2VSIM. In C2VSIM, surface water deliveries are used first to meet demand, and any deficit in surface water supply is then met by pumping groundwater.

3.3 Climate models and crop and hydrologic scenarios

To account for the uncertainty associated with future projections from different GCMs, we performed a preliminary analysis to select suitable climate models for this study. We compared the empirical cumulative distribution functions (ECDFs) of mean annual runoff (VIC-simulated annual total runoff averaged over 2006–2099 for the Sacramento, San Joaquin, and Kings Rivers for RCP 8.5) among different combinations of GCMs (for more information, refer to Text S4 and Fig. S3 of supplementary information). Based on our comparison, we selected 20 GCMs that capture most variability out of the 32 GCMs archived in the Coupled Model Intercomparison Project phase 5 (CMIP5; the selected GCMs are shown in Table S3 of supplementary information). We considered both RCP 4.5 and RCP 8.5 global emissions scenarios. We first ran integrated chain of models for the historical period (1950–2009), where land use and cropping patterns vary annually (referred to as "Hist" hereafter). Next, we ran the models with historical climate (1950–2009) and assumed fixed (to 2003 levels) agricultural practices and cropping patterns (referred to as "Baseline"). To assess the impact of climate change, we ran the models with future climate forcings (2010–2098) based on projections for RCP4.5 and RCP8.5 (we refer to this simulation as "CCR" hereafter), where we assumed fixed (at 2003 levels) agricultural practices and cropping pattern. We also conducted scenario analyses to examine future climate impact on groundwater storage. We analyzed the simulation results for three future periods: beginning of century (BOC; years 2010–2039), mid-century (MOC; years 2040–2069), and end of century (EOC; years 2070–2098). The formulation of scenarios is detailed in Sections 3.3.1 and 3.3.2 as well as in Table 1.

Table 1 Summary of the scenarios considered in this study

Scenario	Description	Period
Hist	Historical climate and cropping pattern	1950–2009
Baseline	Historical climate and cropping pattern for 2003	1950–2009
CCR	Climate change run (future forcing + 2003 cropping pattern) for RCP 4.5 and RCP 8.5	2010–2098
FC	Future crop water use (CCR forcing over CV + headwater inflows as Hist + 2003 cropping pattern)	2010–2098
FI	Future inflows (Hist forcing over CV + headwater inflows as CCR + 2003 cropping pattern)	2010–2098
I_SC	Headwater inflows seasonality change (seasonality as CCR + mean annual volume as Hist) + 2003 cropping pattern	2010–2098
I_AC	Headwater inflows annual volume change (mean annual volume as CCR + seasonality as Hist) + 2003 cropping pattern	2010–2098
CS	Cropping shift (future forcing + 40% and 60% shift from row to tree crops)	2010–2098

3.3.1 Future crop water use and headwater inflow change scenarios

The amount of groundwater being pumped to meet agricultural demands in the CV is essentially a balance between the crop water demand, precipitation, surface water supply from headwater watersheds, and delta outflow to the Pacific. Crop evaporative demand increases with temperature or, precisely, with temperature-dependent variables such as the vapor pressure deficit, net radiation, and the slope of the vapor pressure relationship with temperature. Historically, crop water demand in the CV has been met primarily by surface water (~ 51%) and groundwater (~ 49%) (Li et al. 2018). As climate continues to evolve, both demand and supply are expected to change, the magnitudes of which will exhibit inter-region variability. In general, there are two main factors that control the CV aquifer response to climate: crop water use (crop evaporative demand) and supply from headwater watersheds. A good understanding of the groundwater changes attributable to these factors is necessary to design proper mitigation measures, as required by SGMA. Here, we conducted two scenario analyses to quantify the relative contribution of these factors to future ΔGW. The scenarios are (1) current crop water use and future inflows (FI) and (2) current inflows and future crop water use (FC). Both the scenarios require current and future input data (inflow and crop water use) of equal time span; however, the historical data spans 60 years (1950–2009) and future data spans 90 years (2010–2099). To solve this issue of varying time length, we generated synthetic time series data that we used as a proxy for current crop water use and headwater inflow. To do so, we randomly sampled the baseline (1950–2009) historical analysis to generate time series of monthly data for 30 years. We repeated the random sampling two more times to create 90 years of data (we used the same 30-year data for each future period for consistency). After performing the experiments, we calculated the change associated with future crop water use (FC) from the difference in CCR and FI, whereas the changes due to future inflow are taken as the difference between the CCR and FC scenarios.

3.3.2 Future headwater inflow volume and seasonality change scenarios

Both the volume (of annual inflow to the CV) and timing (seasonality) of headwater inflows are expected to change in the future. An understanding of the relative contribution of headwater inflow volume and seasonality to groundwater storage change is important to design potential mitigation measures like managed aquifer recharge, as suggested by SGMA.

Moreover, the effects of these projected changes on groundwater storage have not been quantified previously. Here, we conducted two scenario analyses by adjusting the projected inflows to quantify relative importance of headwater inflow volume versus seasonality. We multiplied the projected headwater inflows (2010–2098) by perturbation ratios between projected inflows and historical inflows following Wang et al. (2011) and Miller et al. (2003). The scenarios are described as follows:

Annual inflow volume adjustment We determined annual perturbation ratios (A_c) from the 30-year (1971–2000) historical mean annual inflows (R) and 30-year projected mean annual inflows (R'_c) for three future periods (2010–2039, 2040–2069, and 2070–2099). We then multiplied the projected inflows (R'_{cij}, c= 2010–2039, 2040–2069, and 2070–2099, i = 1, …, 12 for each month, j = 1, . . , 90 years) by these ratios. The modified time series (T_{cij}) consists of inflows that have the same annual mean as historical (1971–2000), but with seasonality as projected for the future period.

$$A_c = \frac{R}{R'_c} \tag{2}$$

$$T_{cij} = A_c \times R'_{cij} \tag{3}$$

The modified inflows (VIC-simulated) corresponding to each GCM were used as input to the CVmod (for CV tributaries where reservoirs exist) or C2VSIM (where no reservoirs exist). We refer to this scenario as I_SC hereafter. The ΔGW attributable to future inflow volume change is later determined from the difference in ΔGW estimated by CCR and I_SC scenarios.

Monthly inflow perturbation We also generated headwater inflow time series that keep the projected annual inflow volumes unchanged in the future, with monthly (mean) fractions of mean annual inflows the same as in the historical period (1971–2000). We determined the mean monthly fractions of annual flows from the 30-year historical period (B_i, i = 1, …, 12 for each month). We then multiplied the projected annual flows (R'_j) by the fractions (B_i) to obtain inflow time series (G_{ij}) with the historical seasonality. Accordingly, the annual volumes remained as projected for the future period.

$$G_{ij} = B_i \times R'_j \qquad i = 1, .., 12; j = 1, .., 90 \tag{4}$$

The modified inflows (VIC-simulated) were used as inputs to the CVmod (for CV tributaries where reservoirs exist) or directly to C2VSIM (where no reservoirs exist). We refer to this scenario as I_AC hereafter. The ΔGW attributable to future inflow seasonality change is later determined from the difference in ΔGW estimated by CCR and I_AC scenarios.

3.4 Cropping pattern scenario

We quantified the ΔGW that is attributable to the historic evolution of crop (area and patterns) from 1950 through 2009. We did this by finding the difference in groundwater storage change estimated from two sets of simulations: (i) crops evolve as they did during the historical period (this is basically the "Hist" simulation) and (ii) crops remain fixed at year 1950 conditions (all

other inputs remain same as "Hist") or Hist_50 hereafter. Moreover, we quantified the climate-related ΔGW during historical period that can come from changing crop water use (as ET changes with climate) and headwater inflow (in the form of seasonality and volume). We estimated historic ΔGW attributable to the change in crop water use (due to climate) from ETo trend, whereas we estimated the effect of headwater inflow change as the difference between total change and crop related changes.

In addition, we quantified the ΔGW that would occur due to a cropping shift from mostly row crops to tree crops (together with future climate). For the scenario analysis, we specified 40% and 60% row crops (classification of row and tree crops based on Xiao et al. 2017) to high water consumptive tree crops (orchard). One motivation behind choosing 40% change is from Xiao et al. (2017), who showed that during 2007–2016, there was an average 40% shift from row crops to tree crops, suggesting that much of the change we "project" has already occurred. In our case, we applied the shift relative to the baseline cropping pattern (year 2003). We ran the models with 40% and 60% crop shifts for all (20) future GCM climate scenarios (referred to as CS hereafter). The difference between the CS and CCR scenarios (ΔGW) is due to a shift from row to tree crops.

4 Results and discussion

4.1 Analysis of historical changes in groundwater storage

Figure 3a, b shows historical (1950–2009) changes in precipitation, headwater inflows, and cumulative changes in groundwater storage (ΔGW). The historical (1950–2009) groundwater depletion rate ΔGW is around 3.0 km^3/year, with interannual variability in that increases during the latter half of the record (1980–2009) due to intermittent wet and dry years (as seen in the precipitation and inflow time series shown in Fig. 3a). For the baseline scenario (2003 cropping patterns), the simulated ΔGW rate is − 3.1 km^3/year. The baseline groundwater depletion rate is slightly higher than the historical rate, mainly due to difference in the historical evolution of land use and cropping patterns; the historical run considers changes (i.e., agricultural area increased monotonically between 1950 and 1975, then became relatively stable), while the baseline run considers land use and cropping patterns to be fixed at 2003 levels.

We compared the simulated ΔGW from C2VSIM with other available estimates. The simulated change (mean trend) in ΔGW for April 2006 to September 2009 from C2VSIM is − 8 km^3/year, compared with − 7.9 ± 1.3 km^3/year by Xiao et al. (2017) and − 7.8 km^3/year by Scanlon et al. (2012). GRACE-based estimates include − 7.2 ± 1 km^3/year by Xiao et al. (2017) and − 6.0 km^3/year by Famiglietti et al. (2011) for the period April 2006 to March 2010 which is also close to our simulated estimate of ΔGW. Figure 3c compares monthly GRACE ΔGW from Xiao et al. (2017) and C2VSIM; it is visually evident that C2VSIM reasonably captures the increasing/decreasing trends.

We estimated the relative contribution of crop water use (evolution of crop area, cropping pattern, and climate-related changes) and headwater inflow change (volume and seasonality) to the historical groundwater overdraft (Section 3.4 discusses the method of separating the individual effects), as shown in Fig. 3d. On average, the relative contribution of crop water use and headwater inflow to ΔGW for the entire CV is around 82% and 18%, respectively. We found that the crop water use–related groundwater loss almost entirely comes from historical

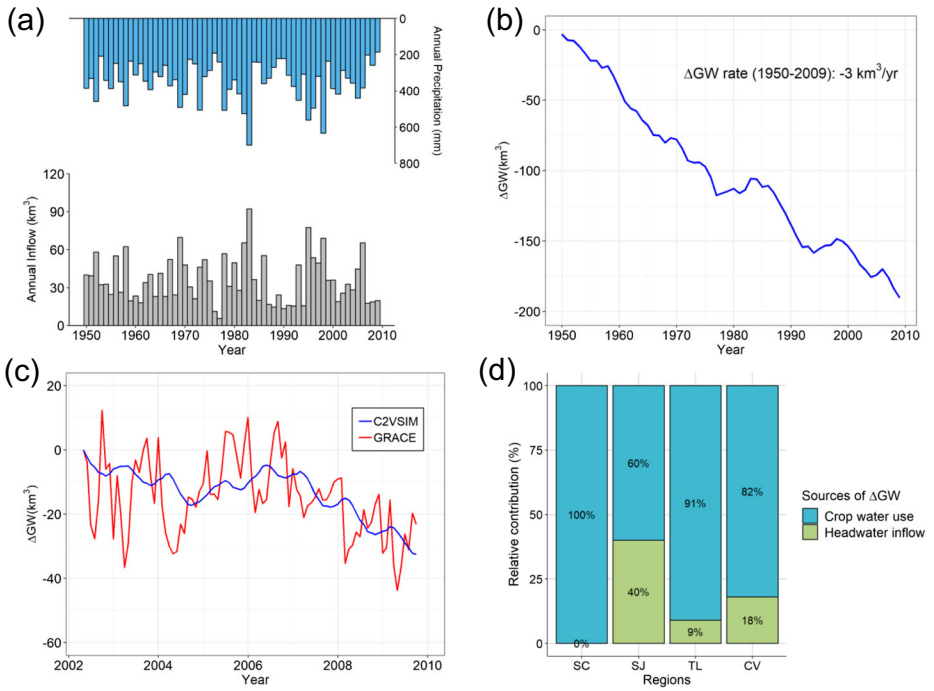

Fig. 3 Historical estimate of annual precipitation and inflows (**a**), annual ΔGW (**b**), ΔGW comparison between C2VSIM simulation and GRACE estimation at monthly time step (**c**), and relative contribution of historical crop water use versus headwater inflow to total ΔGW (**d**)

evolution (increase) in crop area and shift in cropping patterns, whereas climate-related increase in crop water use is negligible (no significant trend exists in reference crop evapotranspiration). Moreover, our region-wide analysis shows that the relative contribution of historical crop evolution and headwater inflow (i) for SC was around 100% and 0%, (ii) for SJ around 60% and 40%, and (iii) for TL around 91% and 9%.

4.2 Changes in hydrology

Figure 4 shows mean annual changes (%) in precipitation (P), headwater inflows (I), and reference evapotranspiration (ETo) for all 20 climate models and scenarios during three future periods (BOC, MOC, and EOC) compared with the historic climate reference period (1971–2000). Multi-model precipitation estimates over CV have a median annual change of −2.2% and −4.4% for RCP4.5 and RCP8.5 respectively near EOC. However, the variability of the multi-model estimates is quite high (standard deviations of 8.9% and 15.2% for RCP4.5 and RCP8.5, respectively). On the other hand, temperature increases in the future will increase crop evaporative demands (here, we have shown ETo change as proxy). Climate change will cause ETo over the CV to increase by 6.6 ± 1.5% and 10.5 ± 1.8% over the CV near the end of the century (EOC) for RCP4.5 and RCP8.5, respectively. The rate of ETo increase is higher in RCP8.5 due to continuing increase in temperature, whereas the rate of increase decreases slightly after mid-century (MOC) in RCP4.5. Additionally, projected changes in temperature and precipitation over the headwater watersheds result in varying impacts on headwater inflows (I). Mean annual inflows have negative trends but high variability especially towards

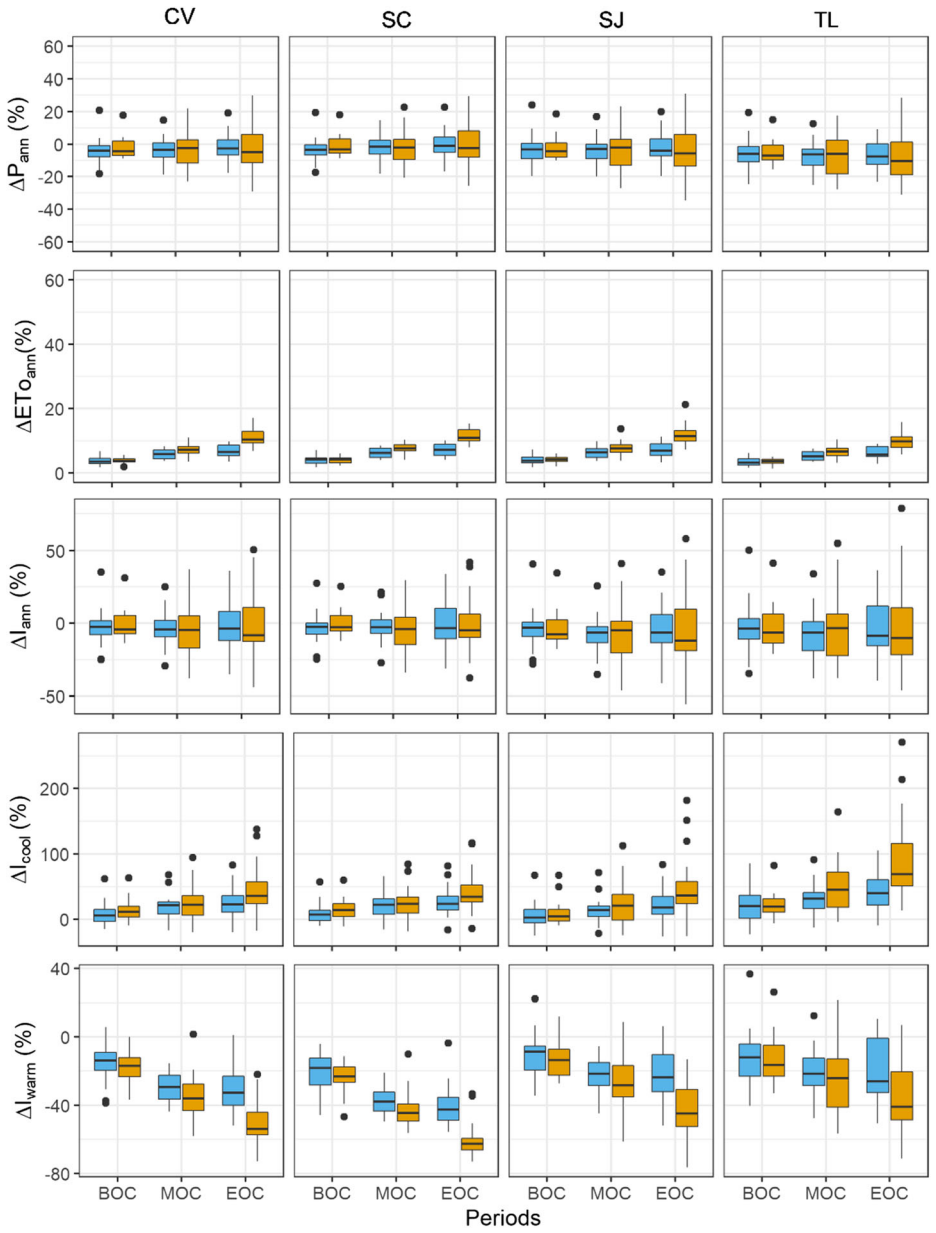

Fig. 4 Changes in annual precipitation (P_{ann}), ETo, and headwater inflow (I_{ann}) in CV and major regions for three future periods relative to 1971–2000. Seasonal variations in inflows are shown in the bottom two rows (sky blue, RCP4.5; brown, RCP8.5). Horizontal axis represents three future periods—beginning of century (BOC; 2010–2039); middle of century (MOC; 2040–2069); end of century (EOC; 2070–2098)

the end of the century, with changes of $-4.20\% \pm 12\%$ and $-4.37\% \pm 19\%$ at MOC and $-3.59\% \pm 16\%$ and $-8.19\% \pm 23\%$ at EOC for RCP4.5 and RCP8.5, respectively (changes of hydrologic variables are shown in Table S4 of supplementary information).

Headwater inflow changes can be both positive and negative (in contrast to ETo which increases in all models). The variability (standard deviation) of future inflow changes is higher than the median in all cases; the headwater runoff projections range from negative to positive depending on the GCM. Moreover, there is a contrasting trend in the cool season (October through March) versus the warm season (April through September) flows where cool season flows are expected (in the median) to increase, and warm season flows are expected to decrease. The variability in multi-model estimates increases towards the end of century (percentage changes in seasonal inflows are shown in Fig. 4). The median changes in annual inflows are negative; this is dominated by warm season decreases versus cool season increases (volumetric changes in inflow are shown in Fig. S4 of supplementary information). To get an idea of multi-model agreement as to the sign of the median change, we calculated the number of concordant minus discordant pairs, divided by the numbers of pairs for annual precipitation and annual and seasonal inflows (shown in Fig. S5 and Fig. S6 of supplementary information). We found that there is little agreement in the annual estimates of inflows (concordance 0.1–0.3) and precipitation (concordance 0.1–0.6, lowest during EOC) among models over the CV. There is, however, greater agreement at the seasonal level of inflow changes (concordance in warm season 0.9–1 and cool season 0.4–0.9). On average, concordance for decreases in inflow during the warm season is higher than for increases in inflow during the cool season.

At the regional level, changes in precipitation are smaller (in absolute value) in the Sacramento than in the San Joaquin and Tulare, where variability across GCM is also larger (Fig. 4). Similarly, mean annual runoff decreases in SJ and TL, whereas there is no clear trend in the multi-model median for SC (percent changes in annual volume are higher in TL and SJ than in SC). However, the multi-model median of headwater inflows in all the regions increases during the cool season and decreases during the warm season, with a high degree of concordance in both measures.

4.3 Projected climate change impacts on groundwater storage

We quantify ΔGW for the projection period (2010–2098) where the forcings come from 20 climate models and 2 RCP scenarios. Figure 5a shows ΔGW for the entire CV and its major hydrologic regions (ΔGW time-series for each climate model are shown in Fig. S7 of supplementary information). It is visually evident that in both RCP scenarios, the CV is expected to go through continuous groundwater depletion with higher multi-model variability towards the end of the century. Median ΔGW at the end of the century (2098) is expected to be -373 ± 88 km^3 for RCP4.5 and -406 ± 116 km^3 for RCP8.5. Furthermore, we fit linear regressions and estimated trends in ΔGW over the future periods (Fig. 5b). The long-term (2010–2098) median (over GCMs) trend in ΔGW is -4.1 ± 1.1 km^3/year for RCP4.5 and -4.4 ± 1.4 km^3/year for RCP8.5, respectively. These represent median trend increases of 31% and 39% compared with the baseline trend (2003 cropping patterns) for RCP4.5 and RCP8.5, respectively. The rate of depletion and uncertainty is higher during EOC, with a median rate ΔGW of -4.4 ± 1.1 km^3/year (RCP4.5) and -4.9 ± 1.4 (RCP8.5) km^3/year, which is equivalent to increases by 40% and 56% increase in ΔGW depletion rate compared with the baseline trends (2003 cropping patterns), respectively. Overall, there will be 40–70% increase (interquartile range of all percent changes) in groundwater depletion over the entire CV.

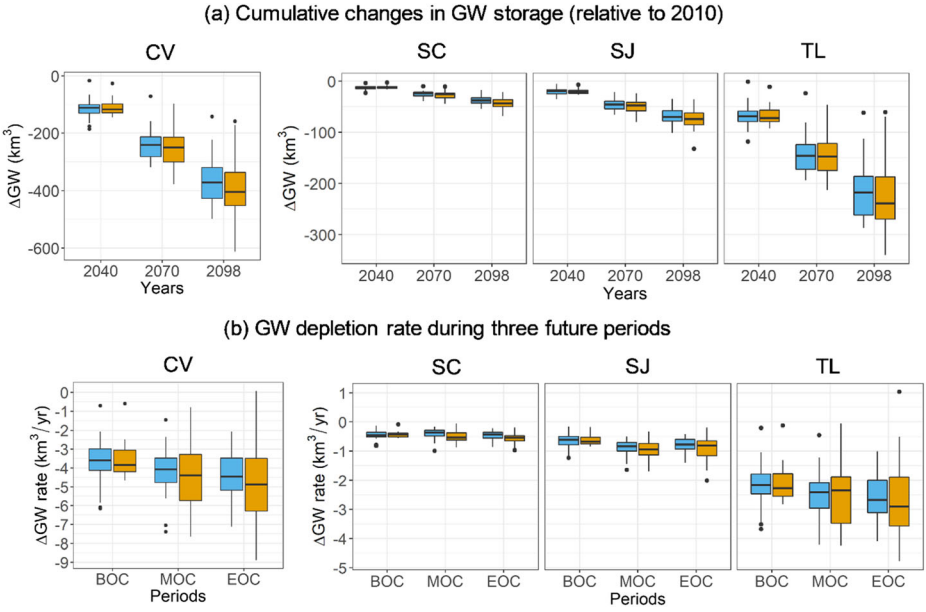

Fig. 5 **a** ΔGW (relative to 2010) in CV and major regions for RCP4.5 (sky blue) and RCP8.5 (brown). The boxplots represent ΔGW obtained by forcing the chain of models with forcing from 20 climate models (ΔGW till 2040, 2070, and 2098 reported in the plot). **b** ΔGW rate during three future periods. Whiskers represent min (max) value or 1.5 times interquartile range from first (third) quartile, whichever is bigger (smaller)

The rate of groundwater decline under future climate change scenarios is not uniform across the CV. The southernmost part (the TL region) will experience higher groundwater declines compared with the central and northern parts (SJ and SC). On average, due to future climate conditions, TL will experience 88% more groundwater decline than either SJ and SC. Separating the results according to the major hydrologic regions of CV, median rates of change in ΔGW in TL during the projection period are -2.5 ± 0.7 km^3/year (RCP4.5) and -2.5 ± 0.9 km^3/year (RCP8.5), which is equivalent to 26% and 28% increases in ΔGW depletion rate compared with the baseline trends (-2.0 km^3/year) for RCP4.5 and RCP8.5 respectively in TL. The second highest depletion is expected in SJ where long-term rates of ΔGW change are -0.78 ± 0.2 km^3/year (RCP4.5) and -0.86 ± 0.3 km^3/year (RCP8.5), which are equivalent to 49% and 65.7% increases in ΔGW depletion rate compared with baseline (-0.52 km^3/year) for RCP4.5 and RCP8.5, respectively. ΔGW in SC is even smaller, with a rate of change in ΔGW expected to be -0.38 ± 0.11 km^3/year (RCP4.5) and -0.48 ± 0.14 km^3/year (RCP8.5), which is an increase in ΔGW depletion rate by 31.3% and 63.5% compared with baseline (-0.29 km^3/year) for RCP4.5 and RCP8.5, respectively. Groundwater losses (in absolute value) are higher for all regions at the end of century (2070–2098) and higher for RCP8.5 than for RCP4.5. In particular, the median (over GCMs) ΔGW rates will increase by 44.4%, 47.1%, and 33.3% respectively under RCP4.5 and 80.9%, 53.9%, and 47.5% for SC, SJ, and TL, respectively, under RCP8.5 at the end of century (regional time series of ΔGW are shown in Fig. S8 of supplementary information).

There are three main elements of the climate change contribution to groundwater storage: (1) changes (increases) in crop water demand due to warmer temperatures, (2) the effect (mostly negative) of changes in annual mean inflows to the CV, and (3) changes in the seasonality (generally, more flow in winter and less in spring and summer) of the inflows to CV. We discuss these elements in the following sections.

4.3.1 Role of future crop water use versus headwater inflows

We analyzed the effect of changes in the demand (crop water use) versus supply (surface water inflows) component of the CV water budget. Figure 6 shows the annual average ΔGW (additional) between FC (future crop water use) and FI (future inflow) scenarios for three future periods. Here, we first calculated the difference in groundwater anomalies (between CCR and FI or FC) and determined the median of the multi-model ensembles, and then we took the mean of the annual changes for each future period.

In all cases, climate change is expected to increase ΔGW (in absolute value). We found that future crop water use (change) will have a greater (negative) impact on total groundwater storage in the CV than inflow changes (FI) (predominantly during the middle to end of the century under RCP8.5); the relative contributions attributable to FC and FI are around 60% and 40%, respectively. At a regional level, future crop water use will have greater (negative) impact in SC (on average 60% of ΔGW), whereas future inflow will have almost equal or greater (on average 50–60% of change) impact (negative) in SJ (except RCP8.5 during EOC), indicating that the SJ is susceptible to both inflow changes and increased crop water use. However, the changes in groundwater in TL due to future inflow changes and crop water use changes are almost the same at BOC and MOC, and changes (negative) due to crop water use are higher at EOC (on average the relative contribution is 50%). We found similarities in the

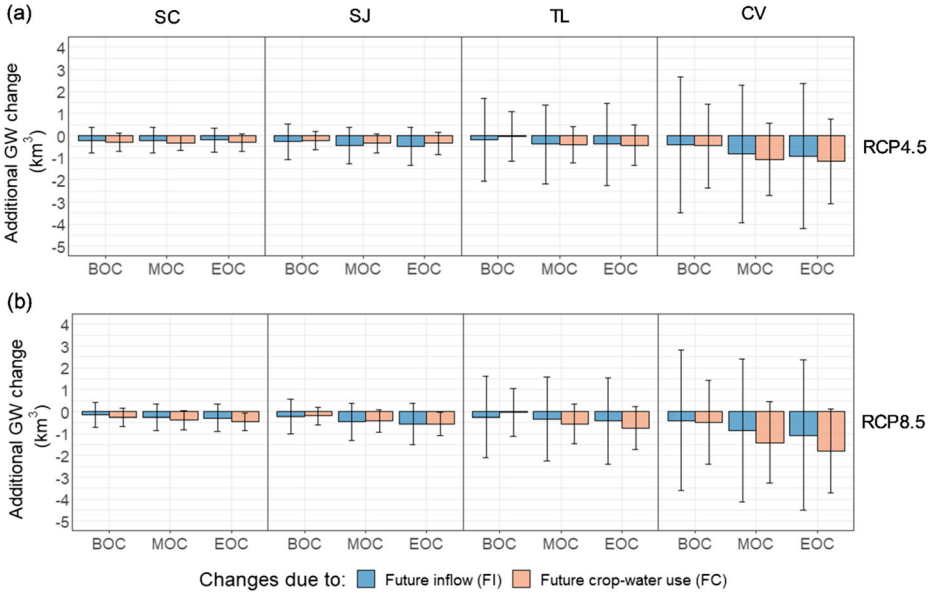

Fig. 6 Additional changes in groundwater storage (annual) due to future crop water use and inflow under RCP4.5 (**a**) and RCP8.5 (**b**) compared with historical (averaged over three future periods). The barplot represents average changes, and the whiskers show the interannual variability (one standard deviation)

relative effect of FI and FC in snow-dominated regions (SJ and TL) as opposed to the rain-dominated region (SC). Our results also indicate that the interannual variability (hence uncertainty) in all cases is higher for FI, which is due to higher uncertainty in inflows (as shown in Fig. 4) and relatively less uncertain future increase in crop water use (because temperature rises in all cases).

4.3.2 Role of headwater inflow volume and seasonality shifts under future climate

Figure 6 shows the effect of FI and FC, where FI is made up of a combination of changes in annual inflow volumes and changes in seasonality. Both effects contribute to ΔGW. To determine the relative magnitude of these effects, we conducted an experiment in which we partitioned the future inflows into seasonal and annual changes (I_SC: seasonality changes in the future, and I_AC: annual volume changes in the future). Figure 7 shows the changes in annual average groundwater storage (additional) due to future inflow seasonality (I_SC) and annual volume (I_AC) (higher negative ΔGW means greater groundwater loss) changes. We followed the same process discussed in the previous section (but between CCR and I_SC or I_AC) and compared the changes (Fig. 7). We found that ΔGW change attributable to FI is about 80% from future headwater seasonality changes and 20% from future annual volume changes. The greatest effect of seasonality changes (more than 80%) is in SC and SJ. On the other hand, inflow volume changes have almost equal effect as seasonality changes in the TL region. We noted that the effects of changes in natural inflows are mediated to varying degrees by headwater regulation; this mediation is much greater for seasonality in contrasted with volume changes. One potential measure to reduce the negative impact of future headwater inflow seasonality is to recharge excess cool season flow through managed aquifer recharge or MAR (DWR Flood-MAR whitepaper). Recent work has shown that Flood-MAR or Ag-MAR

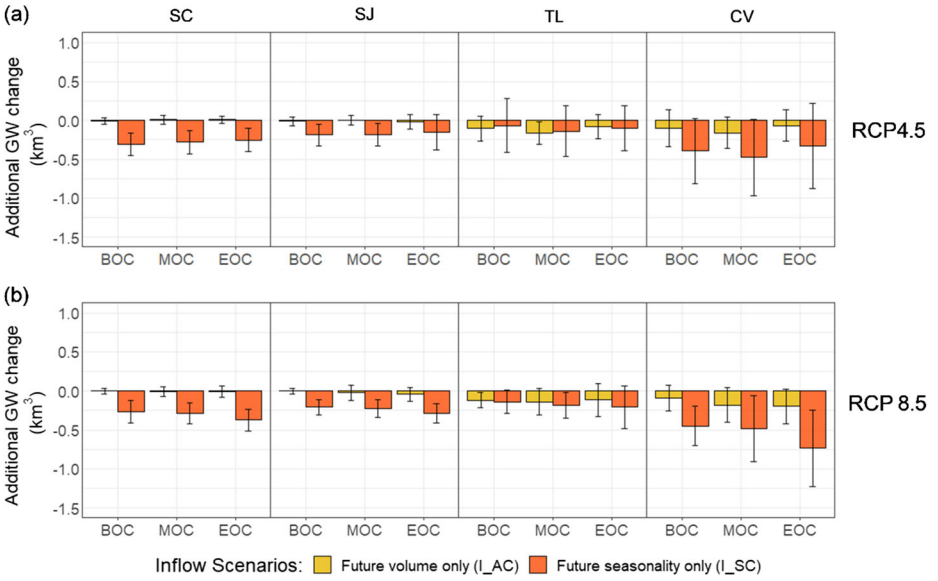

Fig. 7 Additional changes in groundwater storage (annual) due to future inflow volume and seasonality changes for RCP4.5 (**a**) and RCP8.5 (**b**) compared with historical (averaged over three future periods). The barplot represents average changes, and the whiskers show the interannual variability (standard deviation)

can be a promising solution to mitigate the effect of climate change on groundwater storage (Kocis and Dahlke 2017; Gailey et al. 2019; Fogg et al. 2018).

4.4 Crop-shift scenario

We compute the ΔGW associated with a 40% and 60% shift towards tree crops (see Section 3.4) for all climate models (RCP8.5 scenario only). In general, a shift towards tree crops is expected to increase water use requirements, but some of the increased water demand is due to climate change, so we partitioned the climate- and crop change–related components. We found that a 40% shift towards tree crops (compared to 2003) causes an additional 0.91 km^3/year groundwater loss, which is equivalent to a 29% increase in ΔGW (in absolute value) compared with the baseline ΔGW rate. The groundwater depletion rate from the combination of future climate (RCP8.5) and crop-shift (40%) shows that the relative contributions of climate and crop-shift are about 58% and 42%, respectively. However, it is important to note that the 40% shift we considered is with respect to the 2003 cropping pattern. As noted above, much of this shift is already in place as of 2018 (see Xiao et al. 2017). For this reason, we also tested a scenario with 60% crop-shift (row to tree), the results of which are that groundwater declines at a rate of (increase relative to baseline) 1.39 km^3/year (equivalent to 44% increase in groundwater depletion rate relative to the baseline). While the shift towards trees from row crops causes increased groundwater loss in all the major regions, the percentage changes are greatest in SJ (46% and 70% increase for two crop-shift scenarios), and the absolute changes are (by far) the largest in TL (0.55 km^3/year and 0.83 km^3/year for 40% and 60% shifts, respectively).

5 Summary and conclusions

Groundwater plays a critical role in the Central Valley's agricultural production and environment. The vulnerability of groundwater to climate in the Central Valley is evident from the drastic decline of this resource over the past few decades (Xiao et al. 2017), during which average annual groundwater loss has exceeded 3.0 km^3/year. Given this backdrop, our objective was to assess historic changes in groundwater storage and to estimate the additional stress likely to be imposed by future climate change within the CV. Our methodology involved (1) simulation of surface and groundwater in the region using chain of integrated models (C2VSIM, CVmod, and VIC), (2) forcing the models with climate model projections under different climate change scenarios (RCP4.5 and RCP8.5), and (3) simulation experiments for cropping pattern change scenarios. Based on our simulations, we conclude that:

- Groundwater storage in CV has been declining in recent decades (1950–2009) at an average rate of about 3 km^3/year. This decline in groundwater has resulted from a combination of gradual increases in crop water use (82% of the overdraft) due to increased crop area (and shifts towards more water intensive crops) and changes in headwater inflow seasonality and volume (18% of the overdraft in aggregate).
- In the absence of mitigation measures, over the future period (2010–2098), groundwater loss is likely to continue, but at an increased rate. Assuming no (further) change in crop types (relative to 2003), the long-term (2010–2098) rate of groundwater decline in CV under future climate will increase from about 3.0 km^3/year to 4.1 ± 1.1 km^3/year (RCP4.5;

modest greenhouse emission scenario) and 4.4 ± 1.4 km^3/year for RCP8.5 (worst scenario), or 31–39% higher than the base case with 2003 crop patterns.

- Groundwater declines are associated both with (1) increased groundwater pumping due to increased crop water demands associated with rising temperatures (and to a lesser extent, reduced precipitation) and with (2) reduced surface water supply to CV from headwater watersheds. We found that, without mitigating measures, the dominant cause of future groundwater declines will be increase in future crop water use (~ 60% of total change). We noted that the projections of headwater inflow changes are much more uncertain (hence, projection variable) as they are dominantly associated with precipitation changes, whereas projections of crop water use, which are dominated by temperature changes, are less uncertain.
- Groundwater declines, both in the past and projected for the future, are dominated by the Tulare (TL) region, which has accounted for roughly 80% of the historical decline. However, the sensitivities of future groundwater loss to climate-related crop water use and inflow changes are not necessarily greatest in the TL basin.

California's new Sustainable Groundwater Management Act (SGMA) mandates that groundwater depletions be brought into balance. Increases in crop water use and reduced surface water availability associated with climate warming constitute an additional stress on the system; depending on specifics, these additional stresses will increase the current imbalance by one-third to one-half. These additional stresses will need to be addressed by efforts to formulate the sustainable surface and groundwater management strategies that will be required to comply with the mandate of SGMA.

Acknowledgments We are grateful to Dr. Tariq Kadir and Dr. Emin Dogrul from the California Department of Water Resources for technical assistance in the use of C2VSIM. We are also grateful to the kind help from Dr. Alan Hamlet at the University of Notre Dame for his assistance with CVmod.

Funding information The University of California Research Initiatives Award LFR-18-548316 supported this work.

References

Alam S, Gebremichael M, Li R (2019) Remote sensing-based assessment of the crop, energy and water Nexus in the Central Valley, California. Remote Sens 11(14):1701

Allen RG, Pereira LS, Raes D, Smith M (1998) FAO irrigation and drainage paper no. 56. Food and Agriculture Organization of the United Nations, 56(97), Rome, p e156

Bales RC, Molotch NP, Painter TH, Dettinger MD, Rice R, Dozier J (2006) Mountain hydrology of the western United States. Water Resour Res 42(8)

Brush CF, Belitz K, Phillips SP (2004) Estimation of a water budget for 1972–2000 for the grasslands area, central part of the Western San Joaquin Valley, California. US Department of the Interior, US Geological Survey

Brush CF and Dogrul EC (2013) User's manual for the California Central Valley groundwater-surface water simulation model (C2VSim), version 3.02-CG. Bay-Delta Office, California Department of Water Resources

Brush CF, Dogrul EC, Kadir TN (2013) Development and calibration of the California Central Valley groundwater-surface water simulation model (C2VSim), version 3.02-CG. Bay-Delta office, California Department of Water Resources

Cal-Adapt (2018). Cal-Adapt is developed by the Geospatial Innovation Facility at University of California, Berkeley. Data downloaded from https://cal-adapt.org/ Accessed Nov. 2018

California State Legislature (2014) Sustainable groundwater management act. Accessed April 12, 2018. https://www.opr.ca.gov/docs/2014_Sustainable_Groundwater_Management_ Legislation_092914.pdf
CDWR (2016) Estimates of natural and unimpaired flows for the Central Valley of California: water years 1922–2014. Report from California Department of Water Resources
Cooper MG, Schaperow JR, Cooley SW, Alam S, Smith LC, Lettenmaier DP (2018) Climate elasticity of low flows in the maritime western US mountains. Water Resour Res 54(8):5602–5619
Dale LL, Dogrul EC, Brush CF, Kadir TN, Chung FI, Miller NL, Vicuna SD (2013) Simulating the impact of drought on California's Central Valley hydrology, groundwater and cropping. Int J Environ Climate Change 3(3):271–291
Famiglietti JS (2014) The global groundwater crisis. Nat Clim Chang 4(11):945–948. https://doi.org/10.1038/nclimate2425
Famiglietti JS, Lo M, Ho SL, Bethune J, Anderson KJ, Syed TH, Swenson SC, De Linage CR, Rodell M (2011) Satellites measure recent rates of groundwater depletion in California's Central Valley. Geophys Res Lett 38(3)
Faunt CC, Hanson RT and Belitz K (2009) Introduction and conceptual model of the Central Valley, California, in Ground-water availability of California's Central Valley, edited by C. Faunt, U.S. Geol. Surv. Prof. Pap., 1766, 1–56
Flint AL and Flint LE (2007) Application of the basin characterization model to estimate in-place recharge and runoff potential in the basin and range carbonate-rock aquifer system, White Pine County, Nevada, and adjacent areas in Nevada and Utah, U.S. Geol. Surv. Sci. Invest. Rep., 2007–5099, 20
Fogg GE, Goharian E, Gailey R, Maples S, Sandoval Solis S (2018) Water Security, Drought and Climate Change: A California Perspective. AGU Fall Meeting 2018. Web: https://ui.adsabs.harvard.edu/abs/2018AGUFM.H51J1429F/abstract
Gailey RM, Fogg GE, Lund JR, Medellín-Azuara J (2019) Maximizing on-farm groundwater recharge with surface reservoir releases: a planning approach and case study in California, USA. Hydrogeol J 27(4):1183–1206
Garrote L, Iglesias A, Granados A, Mediero L, Martin-Carrasco F (2015) Quantitative assessment of climate change vulnerability of irrigation demands in Mediterranean Europe. Water Resour Manag 29(2):325–338
Gleick PH (2000) Water: the potential consequences of climate variability and change for the water resources of the United States, National Water Assessment Group for the U.S. Global Change Research Program
Hanson RT, Dettinger MD (2005) Ground-water/surface-water responses to global climate simulations, Santa Clara–Calleguas Basin, Ventura County, California, 1950–93. J Am Water Resour Assoc 41(3):517–536
Hanson RT, Flint LE, Flint AL, Dettinger MD, Faunt CC, Cayan D, Schmid W (2012) A method for physically based model analysis of conjunctive use in response to potential climate changes. Water Resour Res 48(6)
ITRC (2003) California crop and soil evapotranspiration for water balances and irrigation scheduling/design. California Polytechnic State University, web: http://www.itrc.org/reports/pdf/californiacrop.pdf
Johnson H (2009) California population: planning for a better future, report, Public Policy Inst. of Calif., San Francisco
Kocis TN, Dahlke HE (2017) Availability of high-magnitude streamflow for groundwater banking in the Central Valley, California. Environ Res Lett 12(8):084009
Li R, Ou G, Pun M, Larson L (2018) Evaluation of groundwater resources in response to agricultural management scenarios in the Central Valley, California. J Water Resour Plan Manag 144(12):04018078
Liang X, Lettenmaier DP, Wood EF, Burges SJ (1994) A simple hydrologically based model of land surface water and energy fluxes for general circulation models. J Geophys Res-Atmos 99(D7):14415–14428
Livneh B, Bohn TJ, Pierce DW, Munoz-Arriola F, Nijssen B, Vose R, Cayan DR, Brekke L (2015) A spatially comprehensive, hydrometeorological data set for Mexico, the US, and southern Canada 1950–2013. Scientific data 2:150042
Massoud EC, Purdy AJ, Miro ME, Famiglietti JS (2018) Projecting groundwater storage changes in California's Central Valley. Sci Rep 8(1):12917
Miller NL, Bashford KE, Strem E (2003) Potential impacts of climate change on California hydrology. JAWRA J Am Water Resour Assoc 39(4):771–784
Miller NL, Dale LL, Brush CF, Vicuna SD, Kadir TN, Dogrul EC, Chung FI (2009) Drought resilience of the California Central Valley surface-ground-water-conveyance system 1. JAWRA J Am Water Resour Assoc 45(4):857–866
Niu GY, Yang ZL, Mitchell KE, Chen F, Ek MB, Barlage M, Kumar A, Manning K, Niyogi D, Rosero E and Tewari M (2011) The community Noah land surface model with multiparameterization options (Noah-MP): 1. Model description and evaluation with local-scale measurements J Geophysical Res: Atmospheres, 116(D12)
Olmstead AL, Rhode PW (2017) A history of California agriculture. Giannini Foundation of Agricultural Economics, University of California

Pierce DW, Cayan DR, Thrasher BL (2014) Statistical downscaling using localized constructed analogs (LOCA). J Hydrometeorol 15(6):2558–2585 -2585

Pierce DW, Kalansky JF, Cayan DR (2018) Climate, drought, and sea level rise scenarios for the fourth California climate assessment. California's fourth climate change assessment, California Energy Commission. Publication number: CNRA-CEC-2018-006

Scanlon BR, Longuevergne L, Long D (2012) Ground referencing GRACE satellite estimates of groundwater storage changes in the California Central Valley, USA. Water Resour Res 48(4)

VanRheenen NT, Wood AW, Palmer RN, Lettenmaier DP (2004) Potential implications of PCM climate change scenarios for Sacramento–San Joaquin River basin hydrology and water resources. Clim Chang 62(1–3): 257–281

Wang J, Yin H, Chung F (2011) Isolated and integrated effects of sea level rise, seasonal runoff shifts, and annual runoff volume on California's largest water supply. J Hydrol 405(1–2):83–92

Xiao M, Koppa A, Mekonnen Z, Pagán BR, Zhan S, Cao Q, Aierken A, Lee H, Lettenmaier DP (2017) How much groundwater did California's Central Valley lose during the 2012–2016 drought? Geophys Res Lett 44(10):4872–4879

Affiliations

Sarfaraz Alam[1] · Mekonnen Gebremichael[1] · Ruopu Li[2] · Jeff Dozier[3] · Dennis P. Lettenmaier[4]

Mekonnen Gebremichael
mekonnen@seas.ucla.edu

Ruopu Li
ruopu.li@siu.edu

Jeff Dozier
dozier@ucsb.edu

Dennis P. Lettenmaier
dlettenm@ucla.edu

[1] Department of Civil and Environmental Engineering, University of California, Los Angeles, CA, USA

[2] School of Earth Systems and Sustainability, Southern Illinois University-Carbondale, Carbondale, IL, USA

[3] Bren School of Environmental Science & Management, University of California, Santa Barbara, CA, USA

[4] Department of Geography, University of California, Los Angeles, CA, USA